Spectroscopy 18 (2004) 13–29
IOS Press


Review

# High resolution nuclear magnetic resonance spectroscopy-guided mutagenesis for characterization of membrane-bound proteins: Experimental designs and applications [1]

Ke-He Ruan

*Vascular Biology Research Center and Division of Hematology, Department of Internal Medicine, University of Texas Health Science Center at Houston, 6431 Fannin St., Houston, TX 77030, USA*
*Tel.: +1 713 500 6769; Fax: +1 713 500 6810; E-mail: kruan@uth.tmc.edu*

**Abstract.** High resolution Nuclear Magnetic Resonance (NMR) spectroscopy is a powerful tool for determining the solution structures of peptides and small proteins, and their ligand binding functions. Molecular biology mutagenesis is a widely used and powerful approach for identification of the protein functions. We have developed a strategy integrating NMR experiments with mutagenesis studies to advance and extend the approaches used for structure/function relationship studies of proteins, especially for membrane-bound proteins, which play important roles in physiopathological processes. The procedures include the design of the functional protein domain, identification of the solution structure and intermolecular contacts between the protein segment and its ligand. These determinations are resolved by high-resolution 2D NMR spectroscopy, and followed by site-directed mutagenesis of the residues suggested from the NMR experiment for the membrane-bound proteins. The residues important to the protein functions, identified by the mutagenesis, were further used to re-assign the NMR spectra and finalize the docking of the protein with its ligand. A structural model of the protein/ligand interaction can be constructed at an atomic level based on the NMR spectroscopy and mutagenesis results. As an application, the strategy has enhanced our knowledge in the understanding of the structure/function relationship for a membrane-bound G protein coupling receptor, the thromboxane $A_2$ receptor (TP receptor), interacting with its ligand, and a microsomal P450, prostacyclin synthase (PGIS), docking with its substrate in the endoplasmic reticulum (ER) membrane. In this review, we have summarized the principles and applications for this newly developed technique.

*Abbreviations*

The abbreviations used are: $TXA_2$, thromboxane $A_2$; TXAS, thromboxane $A_2$ synthase; PGIS, prostacyclin synthase; TP receptor, thromboxane $A_2$ receptor; HPLC, high performance liquid chromatography; NOESY, nuclear Overhauser effect spectroscopy; TOCSY, total correlation spectroscopy; DQF-COSY, double-quantum filtered correlation spectroscopy.

[1]This work was supported by National Institutes of Health (USA) Grants HL 56712 and NS 23327.

## 1. Introduction

Biological functions of proteins are reflected in binding activities, such as an enzyme binding to its substrate and a receptor binding to its ligand. The knowledge of the precise interaction of the protein and ligand at molecular and atomic levels is crucial for the understanding of the action mechanism of the proteins related to the physiopathological processes and structure-based drug designs. Crystallography offers the precise structural determination for crystallized proteins. However, large amounts of active proteins, especially for the membrane bound proteins, could not be crystallized due to hydrophobic properties. NMR spectroscopy offers an alternative way to solve the peptide and protein structures in solution. But the high-resolution NMR technique deals with the normal size of proteins (50 kD and up), which can be difficult because of the slow tumbling of the larger molecules. In addition, the factors included the difficulty of the large-scale expression of the isotope labeled proteins and incorporation of membrane proteins into micelles created a larger sized protein molecule, and therefore limits the high resolution NMR technique for the structural characterization of the membrane proteins. Recently, several novel NMR spectroscopic techniques have been developed to determine the interaction of proteins and ligands [1–13], which include the transferred NOE effect [14–20] and chemical-shift changes [21–25] used to observe the ligand conformation changes upon binding to the protein. However, to identify the residues important to the ligand binding on the membrane proteins in structural terms is still a big challenge for the high resolution NMR spectroscopy. Usually, site-directed mutagenesis is used for screening the functional residues of the protein. But, without structural support, the one by one mutagenesis is not efficient for time frames or resources. In addition, the mutation result might not directly apply to the understanding of the structure/function relationship at molecular and atomic levels because the mutation may result from post-translation changes of the proteins, such as protein folding, glycosylation, membrane incorporation and signaling. To take the advantages of the high resolution NMR spectroscopy, for the determination of the solution structure of the peptide, and site-directed mutagenesis, for the identification of the protein function at a single residue level, and combine the two approaches in a single system might enable the enlargement of the scope and enhancement of the powers of either approach individually. In this review, I introduce a way in my laboratory characterized by the structure/function relationship of membrane proteins using a system connecting the several approaches in one, which includes molecular modeling, constrained peptide synthesis, NMR structural determination, and site-directed mutagenesis. The general experimental designs and applications are summarized below.

## 2. General experimental designs

The concept of high resolution NMR spectroscopy-guided mutagenesis is to combine the advantages of the NMR technique, in understanding the detailed molecular structure of the peptide and the site-directed mutagenesis, in understanding the detailed molecular function of the protein. The general steps involved in the experimental designs are summarized in Fig. 1. As a brief description, the portion of the membrane protein of interest shall be synthesized in an appropriate size for NMR spectroscopic studies and a conformation mimicking the portion of the native protein, based on the molecular modeling, should be constrained using spacers. After the biological test for activity of the constrained peptide mimicking the membrane protein function, high-resolution 2D NMR spectroscopy shall be used to determine the solution structure of the peptide. Then, the function of the peptide interacted with other molecules, such as its ligand, should be investigated by analysis of the 2D spectra for the peptide in the presence of its

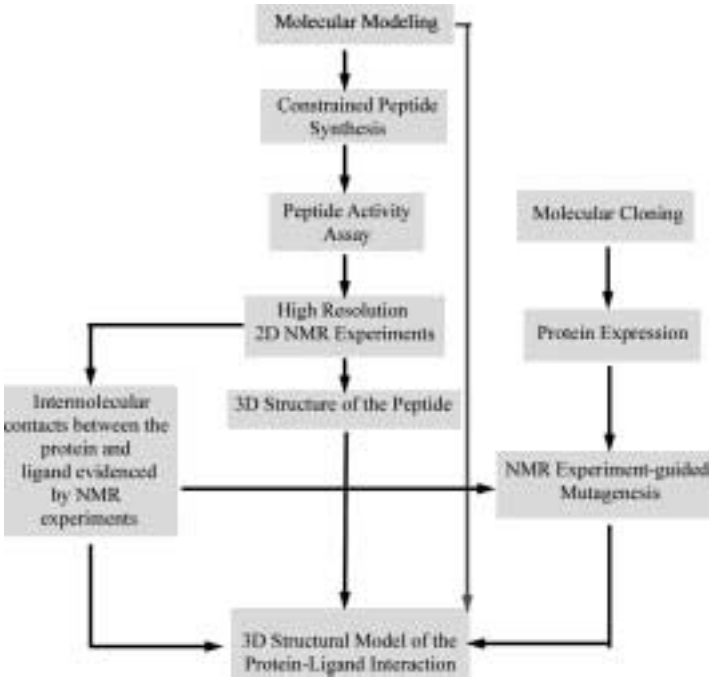


Fig. 1. The general steps involved in the experimental designs for the high resolution NMR spectroscopy-guided mutagenesis.

ligand. The next step is to localize the ligand contacted residues on the native membrane-bound proteins by the site-directed mutagenesis approach, based on the NMR experiments-suggested residues. And then the mutation results can be used to revise and refine the NMR assignment. Finally, the protein ligand interaction site can be constructed in 3D structural terms by structural calculations using the mutation results and NMR constraints.

### *2.1. Molecular modeling*

In order to design an appropriate conformation for a targeted portion of the protein, in which 3D structure is not available, molecular modeling is used as a way to help understand the backbone of the targeted fragment. The Insight II protein modeling package is suitable software for molecular modeling on a Silicon Graphics (SGI) workstation. The detailed approaches used for our successful protein modeling of thromboxane $A_2$ synthase (TXAS) [26,27], prostaglandin $H_2$ synthase (PGHS) [28], PGIS [29], and the TP receptor [30] can be used as references.

### *2.2. Computation-guided constrained peptide synthesis*

3D crystal structures or NMR solution structures of the proteins are ideal models for designing the portion of interest from the protein with similar configurations in the native protein. However, most of the membrane proteins do not have 3D structures at this time. In this case, the working model created by homology modeling, using existing 3D structures of other similar molecules as a template, can be used as a initial experimental design. A peptide mimicking the target domain of the membrane protein with secondary structural configuration can be synthesized. The size of the peptide is based on the feasibility of the NMR experiments. Expression of the peptide using a molecular biology approach is

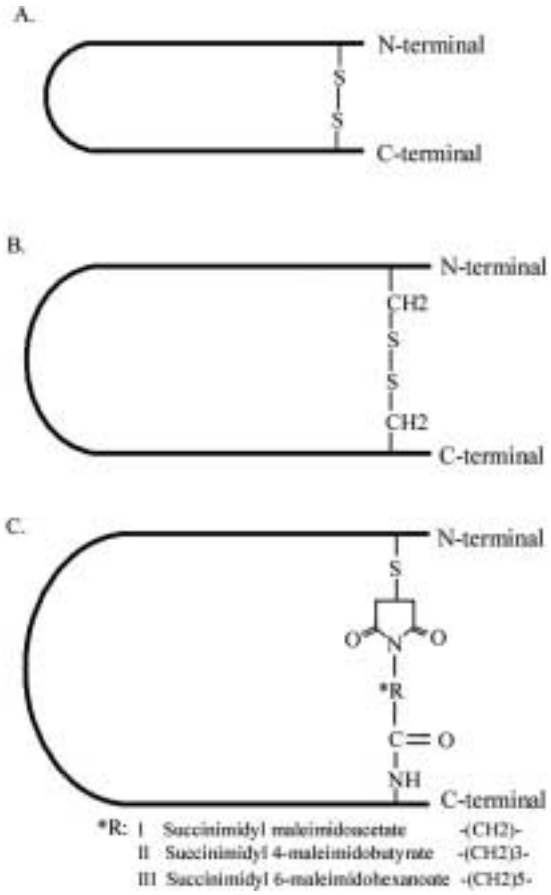


Fig. 2. Constrained peptide designs. A synthetic peptide mimicking a portion of a protein can be constrained to a loop peptide with different distances between the N- and C-termini by introducing different linkers, such as a disulfide bond using cysteine (A), homocysteine (B), or a maleimide compound (C) of different sizes (shown as $^{*}$R).

also feasible. To constrain the peptide into an active form with a certain configuration, a spacer with a defined distance, matching the distance predicted from the structural model, can be used to connect the termini. For example, for a loop configuration of the peptide, Cys or homoCys disulfide bonds can be introduced to the peptide termini to give a 5–12 Å separation of the termini (Fig. 2). For a longer separation, maleimide directives can be introduced to connect the peptide termini. In the later case, the NH-group of the side chain should be used for the melaimide group coupling. Special attention is required for this type of peptide synthesis.

### *2.3. Configuration of the peptide into active form*

Two general methods used in my lab to configure the synthetic peptides are described here.

#### *2.3.1. Cyclization of the synthetic peptide by disulfide bond formation*

The synthetic peptides, with Cys or homoCys added at the peptide termini, were purified to homogeniousity. The formation of the disulfide bond to bring the peptide into the designed configuration can be achieved by oxidation of the peptide in a standard method [31]. The peptide monomer needed to be

dissolved in 1 ml DMSO, and added into $H_2O$ at a final concentration of 0.02 mg/ml. The solution was adjusted to pH 8.5 using trifluoroethylamine dimethyphamarmide, and stirred at room temperature for 24–48 hours. The constrained peptide by the oxidation was lyophilized and purified by HPLC on the C4 column [32].

*2.3.2. Maleimide–Cys coupling*

In general, different lengths of maleimide compounds, introduced to the side chain of the N-terminal amino acid during peptide synthesis, are used for coupling to Cys located in the C-terminal position. After cleavage of the peptide from resin, and removal of the protection group from the thiol group of Cys, the maleimide–Cys coupling can be completed by bringing the pH to 6–7 for 24 hours [33–40].

### *2.4. Biological activity of the engineered peptides*

Before performing time-consuming high-resolution NMR spectroscopic experiments, the biological activity of the protein fragment should be tested. The suitable approaches for the activity identification can be spectroscopic studies, such as circular dichroism (CD), fluorescence spectroscopes, and peptide binding assays, and signaling assays. CD and fluorescence experiments are especially useful because the approach is easy and the experimental conditions can be adopted for further NMR spectroscopic studies, and secondary structural observations in CD spectroscopy can be used as a structural reference for the NMR experiments.

### *2.5. NMR measurements*

In my laboratories, NMR measurements for the constrained peptides were done in $H_2O$ or in $D_2O$ (10%). 2D $^1$H NMR spectra, double-quantum-filtered correlation spectroscopy (DQF-COSY), total correlation spectroscopy (TOCSY) and nuclear Overhauser effect correlation spectroscopy (NOESY) with various mixing times, were obtained at 10–30°C in a 1 mM phosphate buffer pH 6.0–6.5. All spectra were accumulated in a phase sensitive manner using time-proportional phase incrementation for quadrature detection in the F1 [41]. Bruker Avance 600 or 800 MHz spectrometer was used to obtain these spectra. The successful NMR experiments used for the determination of the synthetic peptides of TXAS [41], PGIS [42,43], and the TP receptor [30,31,44] can be adopted for most of the constrained peptide studies.

### *2.6. NMR spectra analysis*

The approaches used for the NMR spectrum analysis and assignments have been described [30,31, 45]. In brief, NMR data processing and proton resonance assignments for the peptides were carried out using the Felix 2000 and up programs, which are installed in SGI workstations. Assignments were accomplished by the combined analysis of the various 2D $^1$H NMR spectra data sets using the standard sequential assignment techniques [45] and the automatic assignment program using the Felix 2000 program [41,45]. Concisely, the proton assignment procedure is based on initial identification of individual spin systems, followed by the correlation of adjacent spin systems along the peptide backbone. 2D DQF-COSY experiments in $H_2O$ solution established NH–C$\alpha$H coupling connectivities, while the COSY in $D_2O$ solution established C$\alpha$H–C$\beta$H and C$\beta$H–C$\gamma$H coupling connectivities of individual spin systems. 2D NOESY experiments in $H_2O$ established space connectivities between the NH proton of residue $i+1$ and NH, C$\alpha$H and C$\beta$H protons of residue $i$. It was thus possible to "walk" down the peptide from the N-terminus to the C-terminus, assigning the NH, C$\alpha$H, C$\beta$H, and C$\gamma$H proton resonances to specific amino acid residues in the sequence [41,45].

### *2.7. NMR structure reconstruction*

Computational and graphic programs required for the proposed structural reconstruction, such as QUANTA-CHARMm/XPLOR/NMR and Insight II, were used in my laboratory. Quantitative analysis of the NMR data provides structural information that can be used as input restraints for structure reconstruction algorithms of distance geometry or molecular dynamics [30,31,41–44,46–49]. The initial structure can be generated via protein modeling and distance geometry approaches based on the qualitative NMR data. The steps involved in the 3D structure construction and refinement can follow the methods described [30,31,46].

### *2.8. Site-directed mutagenesis*

We have established standard mutagenesis methods for our membrane proteins of interest, such as PGIS (one of the microsomal P450 enzymes), and the TP receptor (one of the G protein coupling receptors). The mutants were constructed using the standard PCR method [46,50,51]. The pcDNA3.1 vector containing either wild type PGIS or TP receptor cDNA was used as a template for the PCR amplification. Two synthetic oligonucleotide primers containing the desired mutation for the receptor were complementary to opposite strands of the template, and extended during the temperature cycling of 95°C for 0.5 min, 53–62°C for 1.5 min, and 68°C for 13 min with a total of 25 cycles using *Pfu* DNA polymerase. The products were then digested with the restriction enzyme *Dpn*I for 1 hour to remove native wild-type strands, leaving only the synthesized mutant strands. The PCR products were then used to transform competent XL1-blue cells, followed by DNA extraction from the selected clones. All mutant constructs were confirmed through DNA sequencing. The plasmid was then prepared using the Midiprep kit for transfection into COS-7 or COS-1 cells.

### *2.9. Expression of PGIS and the TP receptor*

The recombinant PGIS or TP receptor protein was expressed in COS-7 or COS-1 cells as described [50,52–55], with some modifications. In brief, COS-7 or COS-1 cells were cultured in high glucose Dulbecco's modified Eagle's medium containing 10% fetal bovine serum and antibiotics. The cells were placed on 100-mm dishes at a density of $1.0 \times 10^6$ and were cultured overnight, and then transfected with the plasmid vectors (pcDNA3.1) constructed with the PGIS or TP receptor cDNA (10–16 $\mu$g/dish) by the DEAE-Dextran plus chloroquine method [46,55] or by the Lipofectamine method [54] following the manufacture instructions. Approximately 48 hours after transfection, the cells were harvested for further protein purification.

### *2.10. Protein activity assay*

#### *2.10.1. Ligand binding assay for the TP receptor*

Ligand binding assays for the wild type and mutants of the TP receptors were performed using the methods described [50,52,56–59]. Briefly, the cell membrane (0.1 mg) in binding buffer was incubated with 1–3 nM of an isotope-labeled TP receptor ligand, [$^3$H]-SQ29,548, at room temperature for 40 min. The reaction was terminated by the addition of 5 ml of ice-cold washing buffer (0.025 M Tris-HCl, pH 7.4). The unbound ligand was then filtered through a Whatman GF/B glass filter under a vacuum. The radioactivity of the receptor-bound [$^3$H]-SQ29,548 remaining on the filter was counted in 10 ml of scintillation cocktail using a Beckman $\beta$ Counter. The radio-binding assay is suitable for other receptor studies.

#### 2.10.2. Enzyme activity determination for PGIS

The PGIS and TXAS activity assays were started by the addition of $^{14}$C-arachidonic acid (AA) (10 $\mu$M) into a mixture of cell homogenates containing TXAS or PGIS in PBS (100 $\mu$l of total volume), and then stopped with 0.5 ml methanol and 1 M citric acid (4 : 1, v/v). The products, 6-keto-$PGF_{1\alpha}$ (degraded $PGI_2$) or $TXB_2$(degraded $TXA_2$) were extracted, separated by thin layer chromatography (TLC) and quantitated by autoradiogram and $\beta$-counter described [29].

## 3. Applications

We have tested this concept of NMR experiment-guided mutagenesis for the structure/function relationship studies of PGIS and the TP receptor, which represent the super families of microsomal P450s and G protein coupling receptors, respectively.

### 3.1. Characterization of the ligand recognition site for a G protein coupling receptor (GPCR) using NMR experiment-guided mutagenesis

#### 3.1.1. TP receptor modeling and the synthetic peptide mimicking the ligand binding site in the extracellular domain

The TP receptor, as other GPCRs, is composed of three iLPs and three eLPs connecting seven transmembrane (TM) helices. The highly conserved extracellular domains of the prostanoid receptors were found in the second extracellular loop ($eLP_2$), which was proposed to be involved in the ligand recognition. The 3D structural working model of the TP receptor was constructed by a homology modeling approach using the crystal structures of bovine rhodopsin as a template, which is the only GPCR having a crystal structure among the GPCR super family (Fig. 3A). The detailed procedures for the protein modeling involved the use of the Insight II protein modeling package on a SGI workstation, following our successful protein modeling of TXAS [26,27]. The TP receptor model adopted the seven TM segments structure of bovine rhodopsin. However, the extracellular domains of the TP receptor could not be built due to the lack of the conservation with the template molecule. The analysis of the human TP receptor model indicated that about 10–14 Å separates the N- and C-termini of the extracellular loops (Fig. 3A). Synthetic loop peptides whose termini are constrained to this separation are presumably more likely to mimic the native loop structure than the corresponding loop region peptide with unrestricted ends. A peptide corresponding to the $eLP_2$ (residues 173–193) of the human TP receptor was made with the N- and C-termini connected by a homocysteine disulfide bond (Fig. 3B). The constrained $eLP_2$ peptide was able to adopt an active conformation, which was evidenced by the binding of the peptide to the receptor ligand using fluorescence (Fig. 4A) and CD spectroscopic studies [30].

#### 3.1.2. Solution structure of the TP $eLP_2$ segment

The solution structure of the TP $eLP_2$ was determined by NMR spectroscopy. Through 2D $^1$H NMR experiments, complete $^1$H NMR assignments for the 2D spectra, including NOESY, TOCSY and DQF-COSY, and structural construction, the overall 3D structure of the constrained $eLP_2$ peptide was constructed. The structure shows two $\beta$-turns at residues 180 and 185 in the TP $eLP_2$ region (Fig. 4B). The distance between the N- and C-termini of the peptide shown in the NMR structure is 14.2 Å (Fig. 4B), which matched the distance (14.5 Å) between the two TM helices connecting the $eLP_2$ in the TP receptor model (Fig. 3A). This information allowed the NMR structure of the constrained peptide to be grafted onto the $eLP_2$ region of the TP receptor model in a configuration without further modifications

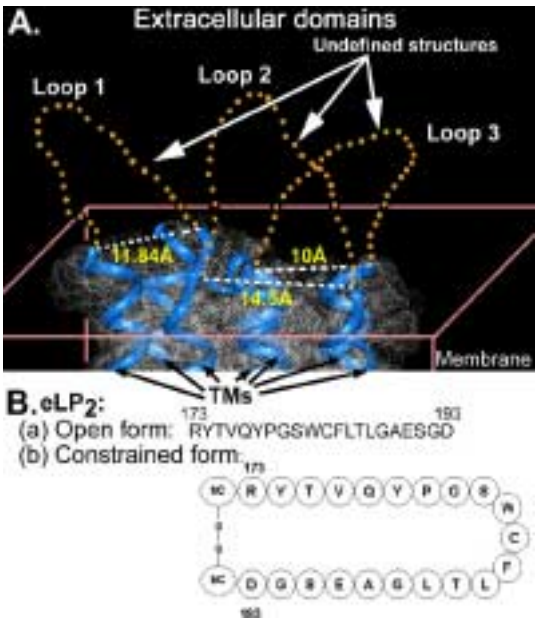


Fig. 3. (A) Seven TM helix model of the human TP receptor based on rhodopsin crystal structure. The undefined eLPs (dotted lines) and the distances between the termini of the eLPs were shown. (B) The sequence of the synthetic TP $eLP_2$ peptide without (a) and with (b) homocysteines (hC) added at each end to form a disulfide bond constrained to the distance of the terminal separation of the $eLP_2$.

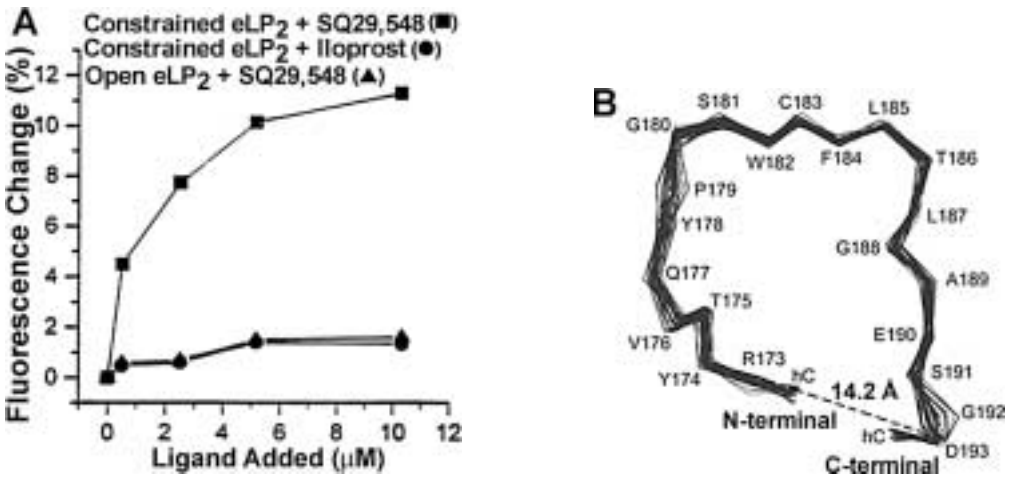


Fig. 4. (A) Fluorescence spectroscopic analysis for the interaction of the receptor ligand with the synthetic TP $eLP_2$. A significant conformation change of the constrained $eLP_2$ induced by SQ29,548 was observed (■) [30]. (B) The 3D NMR structure of the TP $eLP_2$. The distance between the termini was 14.2 Å [30].

(Fig. 5). This study suggests that the approach using the constrained loop peptides greatly increases the likelihood of solving the entire 3D structure of the extra- and intra-cellular domains of the TP receptor and other G protein coupling receptors, which have no crystal structures thus far.

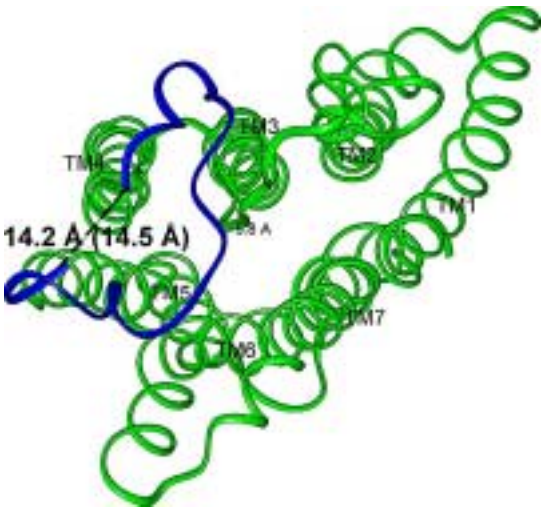


Fig. 5. NMR structure of the $eLP_2$ (dark line) grafted onto the TP receptor model [30].

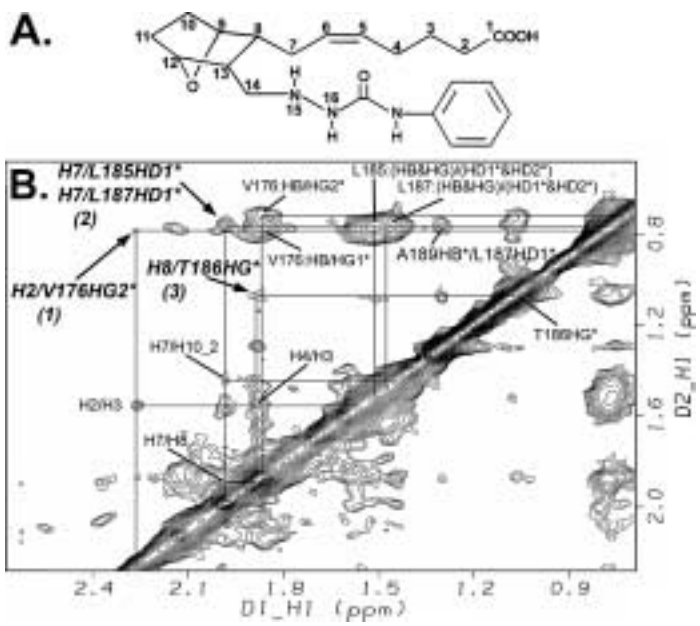


Fig. 6. (A) Chemical structure of SQ29,548. (B) NOESY spectrum of the TP $eLP_2$ with SQ29,548. The NOEs that reflected the contacts between the peptide and SQ29,548 were numbered and indicated with arrows [46].

### *3.1.3. Identification of the ligand recognition site by 2D NMR spectroscopy*

To further identify the residues involved in ligand binding, a TP receptor antagonist, SQ29,548 (Fig. 6A), was used to interact with the synthetic constrained TP $eLP_2$ peptide. High-resolution 2D $^1$H NMR experiments, NOESY and TOCSY, were performed for the peptide, SQ29,548, and the peptide with SQ29,548. Through completed 2D $^1$H NMR assignment and by comparing the different spectra, extra peaks were observed on the NOESY spectrum of the peptide with SQ29,548, which implied the intermolecular contacts between the $eLP_2$ residues (at Val176, Leu185, Thr186, and Leu187) and

SQ29,548 (at position H2, H7, and H8) (Fig. 6B). These results further indicated that the constrained TP $eLP_2$ peptide could adopt an active conformation, and the solution structure of the $eLP_2$ could be a native conformation for the portion of the receptor in bound form. The agreement of the NMR structure of the peptide and the crystal structure of the portion of protein remains to be tested in the future. At least for now, the peptide structure can be used as a model to explain and design the structure related experiments before the crystal structure is available.

### *3.1.4. Site-directed mutagenesis for the important residues contacted with the receptor ligand observed from the NMR experiment*

To determine whether the intermolecular contacts observed from the NMR experiment using the synthetic constrained peptide can be applied to the native receptor protein, site-directed mutagenesis was used to confirm the possible ligand-recognition sites on the human TP receptor. Each of the four residues, Val176, Leu185, Thr186, and Leu187, were mutated to residues in either the same group, with a different structure, or with a different charge. The mutated receptors were then tested for their ligand binding activity. The receptor with the V176L mutant retained binding activity to SQ29,548. All other mutations resulted in a decrease or loss of binding activity to SQ29,548 (Fig. 7A). These mutagenesis results supported the prediction from the NMR experiments in which Val176, Leu185, Thr186, and Leu187 were the possible residues involved in ligand recognition. The constraints of the contacts between the residues in the $eLP_2$ and the protons of SQ29,548, observed in the NMR spectrum, were used to present the ligand/receptor interaction in solution (Fig. 7B). This information facilitates the understanding of the molecular mechanism of $TXA_2$ binding to the important receptor. This integrative approach, combining the NMR experiments and recombinant protein technique for the identification of the residues important to the protein function in structural presentation, was termed “NMR experiment-guided mutagenesis”. In general, this finding provided an alternative way to determine the ligand contact sites for G protein coupling receptors lacking crystal structures.

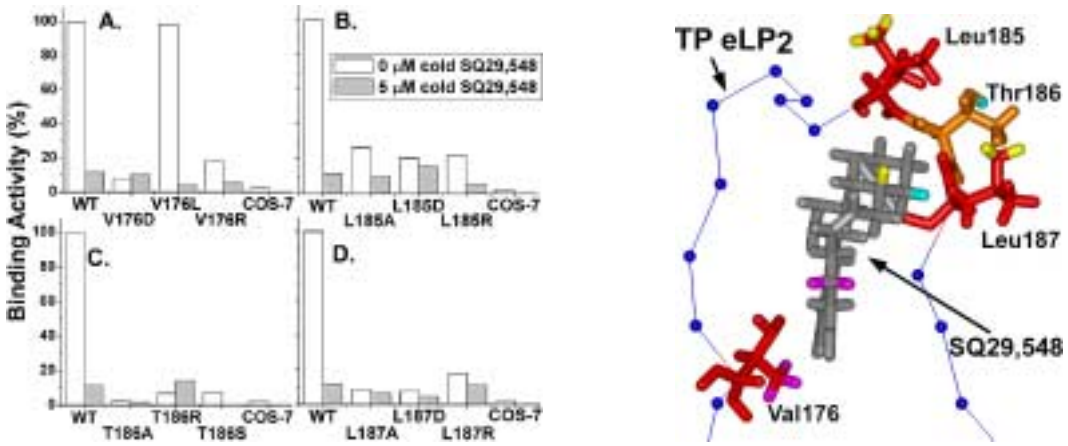


Fig. 7. (A) Binding of the wild type (WT) and the mutant TP receptors (with point mutations at Va1176 [A], Leu185 [B], Thr186 [C] and Leu187 [D] to different residues) to [$^3$H]SQ29,548 without (open bars) and with (shaded bars) the unlabeled SQ29,548 [46]. (B) NMR structure of the TP $eLP_2$ bound with SQ29,548. The ligand-contact residues were displayed with side chains and residue numbers.

### *3.2. Characterization of the substrate docking sites for a microsomal P450, PGIS*

Another large family of membrane proteins is microsomal cytochrome P450 enzymes. We used PGIS, an eicosoniod-synthesizing P450 enzyme as a model for the structure/function relationship studies using the high resolution NMR experiment-guided mutagenesis approach.

#### *3.2.1. Molecular modeling and computation-guided constrained peptide synthesis for the helix F/G loop of PGIS*

Crystallographic structures are known for several soluble bacterial P450s, including $P450_{cam}$ [60], $P450_{BM\text{-}3}$ [61] and $P450_{ter}$ [62]. However, despite the large amount of the microsomal P450 enzymes, there is only one with a crystal structure, an engineered microsomal P450 (P450 2C5) with a deleted N-terminal membrane anchor domain and modified helix F/G loop. The structure offers a template for the molecular modeling of the backbone of other microsomal P450 enzymes. We have constructed working 3D structural models for PGIS [29] (Fig. 8A) based on the crystallographic structure of the engineered P450 2C5 and bacterial $P450_{BM\text{-}3.}$ The overall features of these 3D models of TXAS and PGIS have been supported by our site-directed mutagenesis of several important residues in the predicted substrate- and heme-binding sites [27,29]. Our current studies using modeling-guided site-specific antibodies indicate that three peptide segments (residues 109–127, 353–368 and 411–431), in different surface regions of PGIS, are exposed on the cytoplasmic side of the ER membrane [63]. These data support the topological model in which the bulk of the eicosanoid-synthesizing P450 protein lies on the outside of the ER bilayer. This hypothesis has been supported by our studies using site-specific antibodies

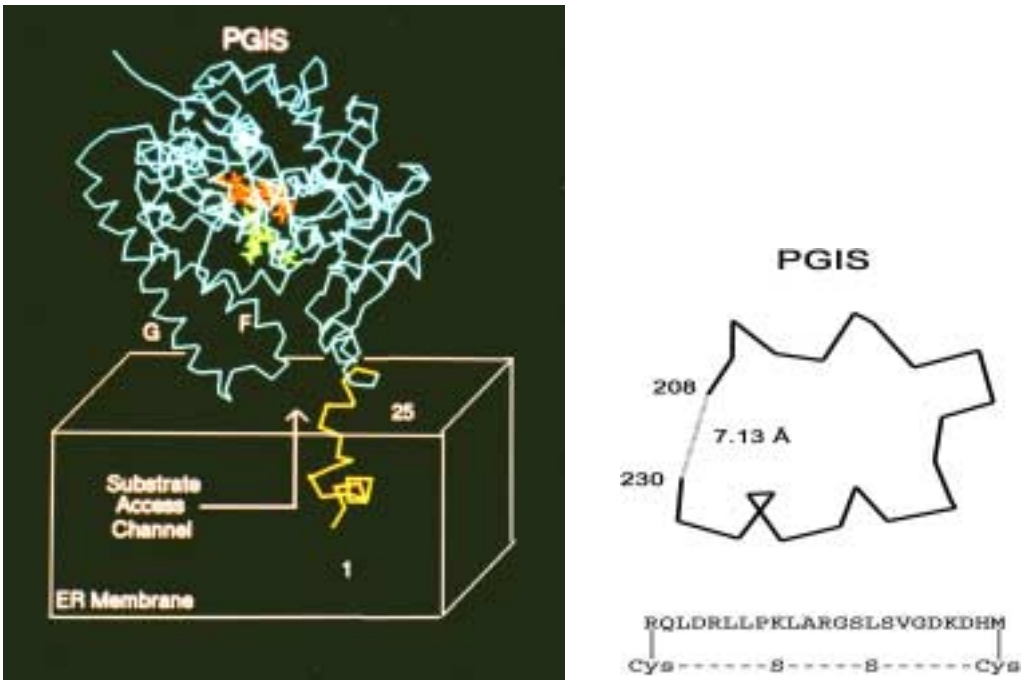


(A) (B)

Fig. 8. (A) Determination of the 3D structure of PGIS F/G loop and identification of its membrane contact residues. (B) Amino acid sequence of the synthetic peptide corresponding to the PGIS helix F/G loop (residues 208 to 230) with cysteines added at both ends of the termini [43].

against peptide segments predicted to be on the surface domains [64] and near the surface of the substrate access channel [65]. The topological model of PGIS has further suggested that the residue(s) within the helix F/G loop of PGIS may be involved in forming the substrate access channel and located in a position that influences the membrane-bound PGIS catalytic function [66]. The distance measured from the model between the F and G helices is about 7 Å (Fig. 8B). We synthesized a peptide to mimic the F/G loop by introducing a Cys disulfide bond to constrain a distance of about 7 Å between the N- and the C-termini of the loop peptide (PGIS residues 208 and 230). We have explored an approach to determine the solution structure and identify the residues of the helix F/G loop important to enzyme activity for the native membrane-bound PGIS by a combination of 2D NMR experiments and mutagenesis methods.

### *3.2.2. Determination of the 3D structure of the helix F/G loop of PGIS by high resolution NMR spectroscopy using the constrained peptide*

The synthesized PGIS F/G peptide was purified by HPLC, and then constrained to a loop conformation by the disulfide bond formation using the method described in Section 2. The corrected molecular weight of the peptide was identified by mass spectroscopy. CD spectroscopy was then used to exam the secondary structure in general, and the detailed 3D structure was determined by 2D $^{1}$H NMR spectroscopy. The peptide was the ideal size for the 2D NMR experiments. We experienced no major difficulty in solving the 3D solution structure of the peptide through the combination of the experiments, TOCSY [67,68], DQF-COSY, and NOESY [69] using a 600 MHz instrument [42].

### *3.2.3. Identification of the residues important to substrate presentation in the F/G loop of the membrane-bound PGIS using high resolution NMR spectroscopy*

So far, no experiment has been used to identify the residues in the F/G loop important to the substrate docking in the eicosanoid-synthesizing P450 enzyme. To test whether the developed NMR experiment-guided mutagenesis is suitable for the detailed studies, after the solution structural determination for the peptide, the interaction of the peptide with the stable PGIS substrate mimic, U46619, was performed. The particular residue of the peptide contacted with the substrate mimic could be identified by the chemical shift changes and intermolecular NOEs, which could be observed in optimal conditions for the spectra. One of the factors was to use the right amount and ratio of the peptide and ligand. Titration of the interaction using the 1D spectrum before the 2D spectrum is highly suggested. We were able to see the intermolecular NOEs and changes of the chemical shifts for the particular residues of the peptide in the concentrations of 10 mg/ml for the peptide and 2 mg/ml for the ligand [43]. Under these conditions, the molar ratio was 1 to 1.43. Once the intermolecular NOEs were identified, the contacts between the peptide and the ligand could be specified at the atomic level. Figure 9 is the example showing the detailed contacts of the two residues in the PGIS F/G loop peptide with U46619 based on the observations of the intermolecular NOEs. It shall be indicated that the intermolecular NOEs could be the NOEs coming from the spin diffusion, and impurities in the peptide, substrate mimic or buffer. A way to exclude this possibility is to subtract the NOESY spectrum of the peptide with the substrate mimic from the negative control spectra of the substrate mimic alone and peptide alone in the same conditions before the intermolecular NOE assignment. We have found out that this is relatively easy for the peptide and small ligand. With increasing the peptide size or using proteins for the interaction, complete exclusion of the possibilities could be difficult.

### *3.2.4. Identification of the residues important to substrate presentation by mutagenesis*

The residues in the F/G loop of PGIS involved for the substrate presentation have not been found before by the observation of the intermolecular contacts between the F/G loop peptide and the substrate mimic in the NMR experiments using the constrained peptide technique. However, the explanation of

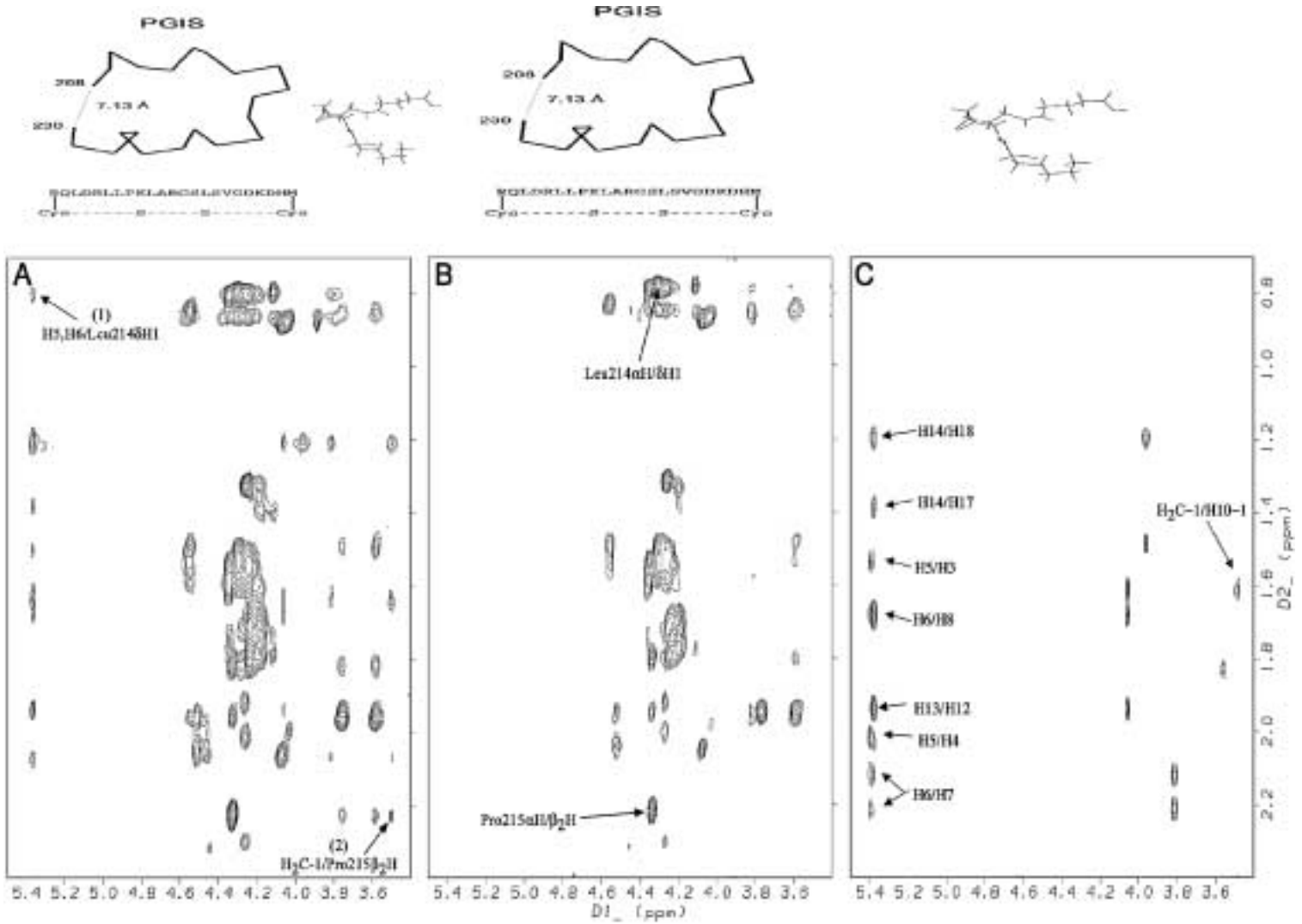


Fig. 9. Expanded region of NOESY spectra of F/G loop with U46619 (A), without U46619 (B) and U46619 only (C) [43]. The extra cross-peaks were identified as the interaction of the F/G loop peptide with U46619: (1) H5 or H6 of U46619 and $\delta_1 H_3$ of Leu214 of the F/G loop; (2) $CH_2$ of U46619 and $\beta$H of Pro215 of the F/G loop (A).

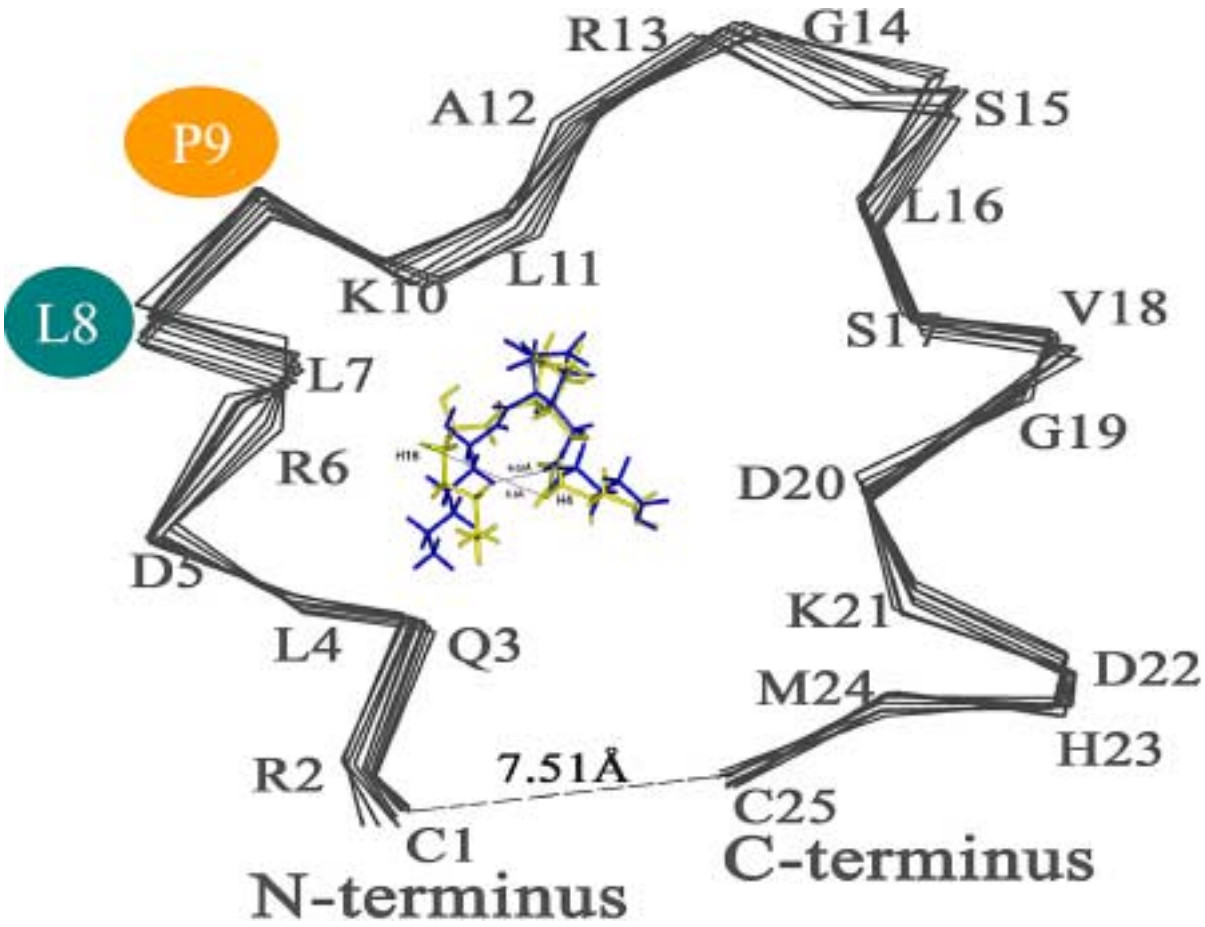


Fig. 10. Superimposition of the 10 best structures using just the $\alpha$-carbons obtained from energy refinement calculations. The distance between the N- and C-terminal is 7.51 Å. The residues (L8, L9) contacted with U46619 were indicated. The conformation changes of U46619 were also displayed.

the NMR structure and the residues of the F/G loop peptide contacted with the substrate mimic from the NMR experiment could be limited by these factors: (1) The peptide segment may not present the full biological activity of the enzyme; (2) The concentrations of the peptide and the enzyme mimic used for the NMR experiment are much higher than the concentrations in the physiological conditions; (3) The biological activities of the native P450 proteins incorporated in the membrane could be different than the peptide in solution. Following the NMR experiment, site-directed mutagenesis for the residues of the parent protein suggested from the NMR experiments was used to address the above questions, which could not be overcome by the NMR technique alone. Through the mapping of the PGIS F/G loop residues based on the effects of the substrate presentation to the membrane-bound PGIS, the mutations of Leu214 and Pro215 were identified to reduce the substrate docking efficiency, which matched the results observed from the NMR experiments (Fig. 10). These results support that the F/G loop is involved in forming the substrate access channel for membrane-bound PGIS and suggests that the NMR experiment-based mutagenesis approach may be applied to study structure and function relationships for other membrane-bound proteins.

## 4. Conclusion

The concept combining molecular modeling, constrained peptide synthesis, high-resolution NMR spectroscopy and site-directed mutagenesis in a system to characterize the structure/function relationship of the membrane-bound proteins has been introduced. The detailed experimental designs and the applications for the G protein coupling receptor and the microsomal P450 enzyme were summarized. Uses of the new strategy have advanced our knowledge in understanding the specific ligand recognition for the TP receptor, and enzyme reaction mechanism for PGIS in solution structural terms at an atomic level. The term, "NMR experiment-guided mutagenesis", was used to describe this concept. It can be used to study other membrane-bound proteins in a wide array of fields. Even several techniques are involved for the studies, but it can be performed in most of the laboratories where there is access to NMR and molecular biology facilities.

## Acknowledgements

We thank Dr. Xiaolian Gao in the Chemistry Department, University of Houston, for access to the NMR facility and providing valuable advice on taking the NMR spectra. We also thank Lori Jenkins and Shui-Ping So for the manuscript editing assistance.

## References

[1] T. Diercks, M. Coles and H. Kessler, Applications of NMR in drug discovery, *Curr. Opin. Chem. Biol.* **5** (2001), 285–291.
[2] M. Shapiro, Applications of NMR screening in the pharmaceutical industry, *Farmaco* **56** (2001), 141–143.
[3] D.J. Craik and M.J. Scanlon, *Annu. Rep. NMR Spectrosc.* **42** (2000), 115–174.
[4] D.C. Fry and S.D. Emerson, Applications of biomolecular NMR to drug discovery, *Drug Des. Discovery* **17** (2000), 13–33.
[5] G.C. Roberts, Applications of NMR in drug discovery, *Drug Discovery Today* **5** (2000), 230–240.
[6] A.K. Ghose, V.N. Viswanadhan and J.J. Wedoloski, *ACS Symp. Ser.* **719** (1999), 226–238.
[7] P.J. Hadjduk, R.P. Meadows and S.W. Fesik, NMR-based screening in drug discovery, *Q. Rev. Biophys.* **32** (1999), 211–240.
[8] J.M. Moore, NMR techniques for characterization of ligand binding: utility for lead generation and optimization in drug discovery, *Biopolymers* **51** (1999), 221–243.
[9] J.M. Moore, NMR screening in drug discovery, *Curr. Opin. Biotechnol.* **10** (1999), 54–58.
[10] M.J. Shapiro and J.S. Gounarides, *Prog. Nucl. Magn. Reson. Spectrosc.* **35** (1999), 153–200.
[11] M.J. Shapiro and J.R. Wareing, NMR methods in combinatorial chemistry, *Curr. Opin. Drug Discovery Dev.* **2** (1999), 396–400.
[12] D.C. Schriemer and O. Hindsgaul, Deconvolution approaches in screening compound mixtures, *Comb. Chem. High Throughput Screening* **1** (1998), 155–170.
[13] P.J. Hajduk, R.P. Meadows and S.W. Fesik, Discovering high-affinity ligands for proteins, *Science* **278** (1997), 497–499.
[14] D. Neuhaus and M.P. Williamson, *The Nuclear Overhauser Effect in Structural and Conformational Analysis*, Wiley–VCH, 2000.
[15] K. Wüthrich, G. Wagner, R. Richarz and S.J. Perkins, Individual assignments of the methyl resonances in the proton nuclear magnetic resonance spectrum of the basic pancreatic trypsin inhibitor, *Biochemistry* **17** (1978), 2253–2263.
[16] N.R. Krishna, D.G. Aggresti, J.D. Glickerson and R. Walter, Solution conformation of peptides by the intramolecular nuclear Overhauser effect experiment, *Biophys. J.* **24** (1978), 791–814.
[17] A. Kumar, R.R. Ernst and K. Wüthrich, A two-dimensional nuclear Overhauser enhancement (2D NOE) experiment for the elucidation of complete proton–proton cross-relaxation networks in biological macromolecules, *Biochem. Biophys. Res. Commun.* **95** (1980), 1–6.
[18] W. Braun, C. Bosch, L.R. Brown, N. Go and K. Wüthrich, Combined use of proton–proton Overhauser enhancements and a distance geometry algorithm for determination of polypeptide conformations. Application to micelle-bound glucagons, *Biochim. Biophys. Acta* **667** (1981), 377–396.

[19] G. Wagner, W. Braun, T.F. Havel, T. Schaumann, N. Go and K. Wüthrich, Protein structures in solution by nuclear magnetic resonance and distance geometry. The polypeptide fold of the basic pancreatic trypsin inhibitor determined using two different algorithms, DISGEO and DISMAN, *J. Mol. Biol.* **196** (1987), 611–639.
[20] A. Bax, Two-dimensional NMR and protein structure, *Annu. Rev. Biochem.* **58** (1989), 223–256.
[21] J. Feeney, G. Batchelor, J.P. Albrand and G.C. Roberts, *J. Magn. Reson.* **33** (1979), 519–529.
[22] J. Feeney, G.C. Roberts, J.W. Thomson, R.W. King, D.V. Griffiths and A.S. Burgen, Proton nuclear magnetic resonance studies of the effects of ligand binding on tryptophan residues of selectively deuterated dihydrofolate reductase from Lactobacillus casei, *Biochemistry* **19** (1980), 2316–2321.
[23] B. Birdshall, J. Feeney, C. Pascual, G.C. Roberts, I. Kompis, R.L. Then, K. Muller and A. Kroehn, A 1H NMR study of the interactions and conformations of rationally designed brodimoprim analogues in complexes with Lactobacillus casei dihydrofolate reductase, *J. Med. Chem.* **27** (1984), 1672–1676.
[24] L.Y. Lian and G.C. Roberts, *NMR of Macromolecules*, G.C.K. Roberts, ed., Oxford University Press, Oxford, 1993, pp. 153–182.
[25] L.Y. Lian, I.L. Barsukov, M.J. Sutcliffe, K.H. Sze and G.C. Roberts, Protein–ligand interactions: exchange processes and determination of ligand conformation and protein-ligand contacts, *Methods Enzymol.* **239** (1994), 657–700.
[26] K.-H. Ruan, K. Milfeld, R.J. Kulmacz and K.K. Wu, Comparison of the construction of a 3-D model bonding pocket, *Protein Engineering* **7** (1994), 1345–1351.
[27] L.-H. Wang, N. Matijevic-Aleksic, P.Y. Hsu, K.-H. Ruan, K.K. Wu and R.J. Kulmacz, Identification of thromboxane $A_2$ synthase active site residues by molecular modeling-guided site-directed mutagenesis, *J. Biol. Chem.* **33** (1996), 19970–19975.
[28] Q.P. Guo, L.H. Wang, K.-H. Ruan and R.J. Kulmacz, Role of Cal509 in time-dependent inhibition of human prostaglandin H synthase-2 cyclooxygenase activity by isoforn-selective agents, *J. Biol. Chem.* **32** (1996), 19134–19139.
[29] S.K. Shyue, K.-H. Ruan, L.-H. Wang and K.K. Wu, Prostacyclin synthase active sites. Identification by molecular modeling-guided site-directed mutagenesis, *J. Biol. Chem.* **272** (1997), 3657–3662.
[30] K.-H. Ruan, S.-P. So, J. Wu, D. Li, A. Huang and J. Kung, Solution structure of the second extracellular loop of human thromboxane $A_2$ receptor, *Biochemistry* **40** (2001), 275–280.
[31] J. Wu, S.-P. So and K.-H. Ruan, Solution structure of the third extracellular loop of human thromboxane $A_2$ receptor, *Arch. Biochem. Biophys.* **414** (2003), 287–293.
[32] K.-H. Ruan, J. Spurlino, F.A. Quiocho and M.Z. Atassi, Acetylcholine receptor–alpha-bungarotoxin interactions: determination of the region to region contacts by peptide–peptide interactions and molecular modeling of the receptor cavity, *Proc. Natl. Acad. Sci. USA* **87** (1990), 6156–6160.
[33] S. Inoue, M. Imagawa, S. Hashida, K.-H. Ruan and E. Ishikawa, A small scale preparation of affinity-purified rabbit Fab'–horseradish conjugate for enzyme immunoassay, *Anal. Lett.* **17** (1984), 229–242.
[34] K.-H. Ruan, S. Hashida, S. Yoshitake, E. Ishikawa, O. Walkisaka, Y. Yamamoto, T. Ichioka and K. Nakajima, A micro-scale affinity-purification of Fab'–horseradish peroxidase conjugates and its use for sandwich enzyme immunoassay of insulin in human serum, *Clin. Chim. Acta* **147** (1985), 167–172.
[35] S. Hashida, K.-H. Ruan and E. Ishikawa, A micro-scale affinity purification of Fab'enzyme conjugates: VTV International Conference on Labeled Antibodies, Tokyo, November, 1985.
[36] K.-H. Ruan, S. Hashida, S. Yoshitake, E. Ishikawa, O. Wakisaka, Y. Yamamoto, T. Ichioka and K. Nakajima, A more sensitive and less time-consuming sandwich enzyme immunoassay for insulin in human serum with less serum interference, *Ann. Clin. Biochem.* **23** (1986), 54–58.
[37] T. Kohno, K.-H. Ruan and E. Ishikawa, A highly sensitive enzyme immunoassay of anti-insulin antibodies in guinea pig serum, *Anal. Lett.* **19** (1986), 1083–1095.
[38] K.-H. Ruan, S. Hashida, K. Tanaka and E. Ishikawa, A small-scale sandwich enzyme immunoassay for macromolecular antigens using beta-D-galactosidase from Escherichia coli and horseradish peroxidase as labels, *Anal. Lett.* **20** (1987), 587–601.
[39] E. Ishikawa, S. Hashida, T. Kohono, K. Tanaka, K.-H. Ruan and S. Ishoue, Enzyme-labeling of antibodies and enzyme immunoassay, in: *Cellular, Molecular and Genetic Approaches to Immunodiagnosis and Immunotherapy*, K. Kano, S. Mori, T. Sugisaki and M. Rorisu, eds, 1987, pp. 116–128.
[40] K.-H. Ruan, D.-R. Ke, S.-W. Hang, D.-R. Ni, S.-Z. Pan, R.-H. Yao, H.-X. Lin and Z.-C. Xie, Determination of insulin in human saliva using a more sensitive sandwich enzyme immunoassay, *Anal. Lett.* **21** (1988), 381–394.
[41] K.-H. Ruan, D. Li, J. Ji, Y.Z. Lin and X. Gao, Structural characterization and topo;ogy of the second potential membrane anchor region in the thromboxane $A_2$ synthase amino-terminal domain, *Biochemistry* **37** (1998), 822–830.
[42] J. Wu, S.-P. So and K.-H. Ruan, Determination of the membrane contact residues and solution structure of the helix F/G loop of prostaglandin $I_2$ synthase, *Arch. Biochem. Biophys.* **411** (2003), 27–35.
[43] H. Deng, J. Wu, S.-P. So and K.-H. Ruan, Identification of the residues in the helix F/G loop important to catalytic function of membrane-bound prostacyclin synthase, *Biochemistry* **42** (2003), 5609–5617.
[44] L. Geng, J. Wu, S.-P. So and K.-H. Ruan, Structural characterization of the first intracellular loop of thromboxane $A_2$ receptor, *Arch. Biochem. Biophys.* (2003), in press.

[45] K. Wüthrich, *NMR of Protein and Nucleic Acids*, John Wiley & Sons, New York, 1986.
[46] S.-P. So, J. Wu, G. Huang, A. Huang, D. Li and K.-H. Ruan, Identification of residues important for ligand binding of thromboxane A2 receptor in the second extracellular loop using the NMR experiment-guided mutagenesis approach, *J. Biol. Chem.* **278** (2003), 10922–10927.
[47] S.-P. So, D. Li and K.-H. Ruan, Identification of the substrate interaction site in the N-terminal membrane anchor segment of thromboxane A2 synthase by determination of its substrate analog conformational changes using high resolution NMR technique, *J. Biol. Chem.* **275** (2000), 40679–40685.
[48] K.-H. Ruan, J. Wu, S.-P. So and L.A. Jenkins, Evidence of the residues involved in ligand recognition in the second extracellular loop of the prostacyclin receptor characterized by high resolution 2D NMR techniques, *Arch. Biochem. Biophys.* (2003), in press.
[49] K.-H. Ruan, S.-P. So, W. Zheng, J. Wu, D. Li and J. Kung, Solution structure and topology of the N-terminal membrane anchor domain of a microsomal cytochrome P450: prostaglandin $I_2$ synthase, *Biochem. J.* **368** (2002), 1–7.
[50] T. Kobayashi, M. Kiriyama, T. Hirata, M. Hirata, F. Ushikubi and S. Narumiya, Identification of domain conferring ligand binding specificity to the prostanoid receptor: studies o chimeric prostacyclin/prostaglandin D receptor, *J. Biol. Chem.* **272** (1997), 15154–15160.
[51] S.M. Miggin and B.T. Kinsella, Investigation of the mechanisms of G protein: effector coupling by the human and mouse prostacyclin receptors. Identification of critical species-dependent differences, *J. Biol. Chem.* **277** (2002), 27053–27064.
[52] C.D. Funk, L. Furci, N. Moran and G.A. Fitzgerald, Point mutation in the seventh hydrophobic domain of the human thromboxane A3 receptor allows discrimination between agonist and antagonist binding sites, *Mol. Pharmacol*. **44** (1993), 934–939.
[53] B.A. Stillman, M.D. Breyer and R.M. Breyer, Importance of the extracellular domain for prostaglandin EP(2) receptor function, *Mol. Pharmacol.* **56** (1999), 545–551.
[54] N. Hatae, K. Yamaoka, Y. Sugimoto, M. Negishi and A. Ichikawa, Augmentation of receptor-mediated adenyl cyclase activity by Gi-coupled prostaglandin receptor subtype EP(3) in a Gbetagamma subunit-independent manner, *Biochem. Biophys. Res. Commun.* **290** (2002), 162–168.
[55] C.M. Gorman, D.R. Gies and G. McCray, Transient production of proteins using an adenovirus transformed cell line, *DNA Protein Eng. Tech.* **272** (1990), 3657–3662.
[56] C.D. Funk, L. Furci, G.A. Fitzgerald, R. Grygorczyk, C. Rochette, M.A. Bayne, M. Abramovitz, M. Adam and K.M. Metters, Cloning and expression of cDNA for the human prostaglandin E receptor EP1 subtype, *J. Biol. Chem.* **268** (1993), 26767–26772.
[57] M. Adam, Y. Boie, T.H. Rushmore, G. Muller, L. Bastien, K.T. McKee, K.M. Metters and M. Abramovitz, Cloning and expression of three isoforms of the human $EP_3$ prostanoid receptor, *FEBS Lett.* **338** (1994), 170–174.
[58] N. Chiang, W.M. Kan and H.H. Tai, Site-directed mutagenesis of cysteinyl and serine residues of human thromboxane $A_2$ receptor in insect cells, *Arch. Biochem. Biophys.* **334** (1996), 9–17.
[59] E.M. Symth, P.V. Nestor and G.A. Fitzgerald, Agonist-dependent phosphorylation of an epitope-tagged human prostacyclin receptor, *J. Biol. Chem.* **271** (1996), 33698–33704.
[60] T.L. Poulos, B.C. Finzel and A.J. Howard, High-resolution crystal structure of cytochrome P450 cam, *J. Mol. Biol*. **195** (1987), 697–700.
[61] K.G. Ravichandran, S.S. Boddupalli, C.A. Hasermann, J.A. Peterson and J. Deisenhofter, Crystal structure of hemoprotein domain of P450BM-3, a prototype for microsomal P450's, *Science* **261** (1993), 731–736.
[62] S.S. Boddupalli, C.A. Hasemann, K.G. Ravichandran, J.Y. Lu, E.J. Goldsmith, J. Deisenhofer and J.A. Peterson, Crystallization and preliminary X-ray diffraction analysis of P450terp and hemoprotein domain of P450BM-3, enzymes belonging to two distinct classes of the cytochrome P450 superfamily, *Proc. Natl. Acad. Sci. USA* **89** (1992), 5567–5571.
[63] Y.Z. Lin, H. Deng and K.-H. Ruan, Topology of catalytic portion of prostaglandin $I_2$ synthase-identification by molecular modeling-guided site-specific antibodies, *Arch. Biochem. Biophys.* **379** (2000), 188–197.
[64] Y. Lin, K.K. Wu and K.-H. Ruan, Characterization of the secondary structure and membrane interaction of the putative membrane anchor domains of prostaglandin $I_2$ synthase and cytochrome P450 2C1, *Arch. Biochem. Biophys.* **352** (1998), 78–84.
[65] H. Deng, A. Huang, S.-P. So, Y.Z. Lin and K.-H. Ruan, Substrate access channel topology in membrane-bound prostacyclin synthase, *Biochem. J.* **362** (2002), 545–551.
[66] P.W. Majerus, Arachdonate metabolism in vascular disorders, *J. Clin. Invest.* **72** (1983), 1521–1525.
[67] L. Braunschweiler and R.R. Ernst, Coherence transfer by isotropic mixing: application to proton correlation spectroscopy, *J. Magn. Reson.* **53** (1983), 521–528.
[68] A. Bax and D.G. Davis, Optimization of two-dimensional homonuclear relayed coherence transfer NMR spectroscopy, *J. Magn. Reson.* **61** (1985), 306–320.
[69] J. Jeener, B.H. Meier, P. Bachmann and R.R. Ernst, Investigation of exchange processes by two-dimensional NMR spectroscopy, *J. Chem. Phys.* **71** (1979), 4546–4553.